Nature of the Chemical Bond between a Transition Metal and a Group-13 Element: Structure and Bonding of Transition Metal Complexes with Terminal Group-13 Diyl Ligands ER (E = B to Tl; R = Cp, $N(SiH_3)_2$, Ph, Me)

Jamal Uddin, Christian Boehme,† and Gernot Frenking*

Fachbereich Chemie, Philipps-Universität Marburg, Hans-Meerwein-Strasse, D-35032 Marburg, Germany

Received November 29, 1999

The equilibrium geometries and first TM−ER bond dissociation energies of 35 transition metal complexes with group-13 ligand atoms $[(CO)_4Fe-ECp]$, $[(CO)_4Fe-EN(SiH_3)_2]$, $[(CO)_5W-EN(SiH_3)_2]$, $[(CO)_4Fe-EPh]$, and $[TM(ECH_3)_4]$ (TM = Ni, Pd, Pt; E = B, Al, Ga, In, Tl) have been calculated at the DFT level of theory using gradient-corrected exchange and correlation functionals (BP86). The bonding situation in the complexes was examined with the help of the NBO and CDA partitioning schemes. The calculations show that the bond energies of the TM−ER bonds are rather high and follow in all cases the trend B > Al > Ga ≈ In > Tl. The TM−ER bonds where R is a poor π-donor (Ph, CH_3) are shorter and stronger than those where R is a π-donating group (Cp, $N(SiH_3)_2$). The NBO analysis of the TM−E interactions indicates that the nature of the TM−ER bond is mainly ionic and that the covalent contributions are less important. The covalent bond order of the TM−ER bonds is always < 1. The TM←ER σ-donation is clearly larger than the TM→ER π-back-donation when R is a strong π-donor. TM→ER π-back-donation becomes larger and may even become bigger than the TM←ER σ-donation when R is a weak π-donor.

1. Introduction

The coordination chemistry of group-13 elements E = B to Tl is presently a topic of intensive experimental research that has led to the successful synthesis of new types of transition metal (TM) compounds.[1] In particular, TM complexes with terminal group-13 diyl ligands ER where the dicoordinated atom E has the formal oxidation state +1 could for the first time become isolated and characterized by X-ray structure analysis. Among the spectacular highlights of experimental research are the first isolation of an terminal alane diyl complex $[(CO)_4Fe-AlCp^*]$,[2] the first examples of stable borylene complexes $[(CO)_4Fe-BCp^*]$[3] and $[(CO)_5W-BN(SiMe_3)_2]$,[4] the synthesis of the "ferrogallyne" $[(CO)_4Fe-GaAr^*]$ (Ar* = 2,6-(2,4,6-triisopropylphenyl)phenyl),[5] and the first homoleptic diyl complexes $[Ni(E-C(SiMe_3)_3)_4]$ with E = In[6] and E = Ga.[7] The latter three examples indicate that even diyl complexes with ligands ER where R is *not* a strong π-donor can become isolated. The experimental studies revealed that the group-13 diyl complexes are remarkably stable and that the difficulty to prepare them lies mainly in the finding of suitable precursor compounds.[2−6] It can be expected that the number of stable compounds of this class will soon become larger.

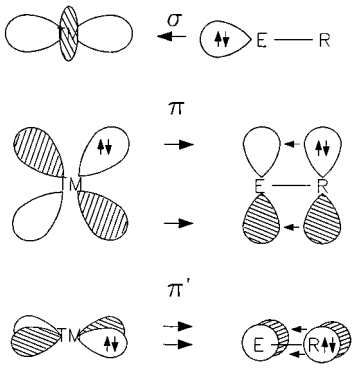

Figure 1. Schematic representation of the TM−E−R bonding situation when R has occupied p(π)-orbitals.

The analysis of the structures and properties of the complexes has led to speculations about the nature of the TM−ER bonds, and some selected molecules have been studied theoretically. The generally accepted bonding model for the TM−ER bond is shown in Figure 1.

† Present address: Université Louis Pasteur, Strassbourg, France.

(1) (a) Irvine, G. J.; Lesley, M. J. G.; Marder, T. B.; Norman, N. C.; Rice, C. R.; Robins, E. G.; Roper, W. R.; Whittell, G. R.; Wright, L. J. *Chem. Rev.* **1998**, *98*, 2685. (b) Braunschweig, H. *Angew. Chem.* **1998**, *110*, 1882; *Angew. Chem., Int. Ed.* **1998**, *37*, 1786. (c) Wrackmeyer, B. *Angew. Chem.* **1999**, *111*, 817; *Angew. Chem., Int. Ed.* **1999**, *38*, 771. (d) Fischer, R. A.; Weiss, J. *Angew. Chem.* **1999**, *111*, 3002; *Angew. Chem., Int. Ed.* **1999**, *38*, 2830.

(2) Weiss, J.; Stetzkamp, D.; Nuber, B.; Fischer, R. A.; Boehme, C.; Frenking, G. *Angew. Chem.* **1997**, *109*, 95; *Angew. Chem., Int. Ed. Engl.* **1997**, *36*, 70.

(3) Cowley, A. H.; Lomeli, V.; Voigt, A. *J. Am. Chem. Soc.* **1998**, *120*, 6401.

(4) Braunschweig, H.; Kollann, C.; Englert, U. *Angew. Chem.* **1998**, *110*, 3355; *Angew. Chem., Int. Ed.* **1998**, *37*, 3179.

(5) Su, J.; Li, X.-W.; Crittendon, R. C.; Campana, C. F.; Robinson, G. H. *Organometallics* **1997**, *16*, 4511.

(6) Uhl, W.; Pohlmann, M., Wartchow, R. *Angew. Chem.* **1998**, *110*, 1007; *Angew. Chem., Int. Ed.* **1998**, *37*, 961.

(7) Uhl, W.; Benter, M.; Melle, S.; Saak, W.; Frenking, G.; Uddin, J. *Organometallics* **1999**, *18*, 3778.

10.1021/om990936k CCC: $19.00
Publication on Web 01/25/2000

There should be strong σ-donation from the electron lone-pair of the electropositive atom E into empty σ-AOs of the transition metal, while TM→ER π-back-donation should be less important because of the low electronegativity of E. The TM→ER π-back-donation would compete with E←R π-donation when R has one or two occupied p(π)-orbitals (Figure 1). It would be important for an understanding of the bonding situation in the complexes if the TM−E and E−R interactions would be analyzed for different elements TM and E and particularly for different substituents R.

Very few theoretical studies about the bonding in TM−group-13 complexes that focused on selected molecules have been published so far. They have shown that the *relative* size of TM←ER σ-donation and TM→ER π-back-donation can be quite different depending on the nature of R. A charge decomposition analysis (CDA)[8] of [$(CO)_4$Fe−AlCp] indicated that the Fe←Al σ-donation is significantly larger than the Fe→Al π-back-donation in this particular compound.[2] The same method revealed, however, that Ni→ECH_3 π-back-donation in [Ni$(EMe_3)_4$] (E = B to Tl) is rather strong.[7] The former complex has an ER group where R is a strong π-donor, while in the latter this is not the case. The X-ray structure analysis of [$(CO)_4$Fe−GaAr*], which also has an ER group where R is a weak π-donor, shows a rather short Fe−Ga bond with a linear Fe−Ga−C_α arrangement.[5] A formulation of [$(CO)_4$Fe−GaAr*] with an Fe−Ga single bond would leave a strongly electron-deficient gallium atom with only four electrons in the valence shell, which is an unlikely valence configuration for a stable group-13 compound. The authors suggested that [$(CO)_4$Fe−GaAr*] should be formulated with an Fe≡Ga triple bond.[5] Thus, the compound would be the first example of a ferrogallyne. This is not an unreasonable suggestion, because the ligand ER is isoelectronic to CR^+, and the bonding situation in Fischer-type carbyne complexes L_nTM−CR, which have TM≡CR triple bonds, can be discussed in terms of donor−acceptor interactions between $L_n$$TM^-$ and CR^+.[9] However, the ligand CR^+ is much more electronegative than ER.

The assignment of an Fe−Ga triple bond in [$(CO)_4$Fe−GaAr*] has been strongly criticized, and on the basis of DFT calculations it was suggested the Fe−Ga bond order is only 1.[10] A recent examination of the bonding situation in [$(CO)_4$Fe−Ga(C_6H_5)] using the CDA method and the natural bond orbital (NBO)[11] partitioning scheme lends some credit to the formulation of an Fe≡Ga triple bond, because the $(CO)_4$Fe→Ga(C_6H_5) π-back-donation was found to be twice as high as in $(CO)_4$Fe→GaCp.[12] However, it was also found that the Fe−Ga bond is dominantly ionic in character, which makes the discussion about the degree of multiple bonding in the remaining covalent part meaningless.

The metal−ligand bonding situation in [$(CO)_4$Fe−L] with L = CO, N_2, SiO, BF, BO^-, BNH_2, and $BN(CH_3)_2$ has recently been investigated in a theoretical study using DFT methods.[27] The authors came to the conclusion that the BR ligands are much better σ-donors than CO and comparable π-acceptors (except BO^-) but that the high polarity of the BR ligands and the buildup of positive charge on BR might lead to a low kinetic stability. Complexes with sterically crowded ligands BNR_2 were suggested as promising candidates for synthesis. This prediction has in the meantime been supported by the successful isolation of the above-mentioned examples.

All previous theoretical investigations of the structures and bonding interactions of group-13 diyl complexes were restricted to selected molecules, and there is clearly a need for a comparative study of the bonding situation of complexes L_nTM−ER with different groups R, ligands L_n, and metals TM for all elements B to Tl. We present the first comprehensive quantum chemical

(8) Dapprich, S.; Frenking, G. *J. Phys. Chem.* **1995**, *99*, 9352.
(9) Vyboishchikov, S. F.; Frenking, G. *Chem. Eur. J.* **1998**, *4*, 1439.
(10) Cotton, F. A.; Feng, X. *Organometallics* **1998**, *17*, 128.
(11) Reed, A. E.; Curtiss, L. A.; Weinhold, F. *Chem. Rev.* **1988**, *88*, 899.
(12) Boehme, C.; Frenking, G. *Chem. Eur. J.* **1999**, *5*, 2184.
(13) (a) Becke, A. D. *Phys. Rev. A* **1988**, *38*, 3098. (b) Perdew, J. P. *Phys. Rev. B* **1986**, *33*, 8822; **1986**, *34*, 7046.
(14) Frenking, G.; Antes, I.; Böhme, M.; Dapprich, S.; Ehlers, A. W.; Jonas, V.; Neuhaus, A.; Otto, M.; Stegmann, R.; Veldkamp, A.; Vyboishchikov, S. F. In *Reviews in Computational Chemistry*; Lipkowitz, K. B., Boyd, D. B., Eds.; VCH: New York, 1996; Vol. 8, pp 63−144.
(15) Hay, P. J.; Wadt, W. R. *J. Chem. Phys.* **1985**, *82*, 299.
(16) (a) Ditchfield, R.; Hehre, W. J.; Pople, J. A. *J. Chem. Phys.* **1971**, *54*, 724. (b) Hehre, W. J.; Ditchfield, R.; Pople, J. A. *J. Chem. Phys.* **1971**, *56*, 2257. (c) Hariharan, P. C.; Pople, J. A. *Mol. Phys.* **1974**, *27*, 209. (d) Hariharan, P. C.; Pople, J. A. *Theor. Chim. Acta* **1973**, *28*, 213. (e) Gordon, M. S. *Chem. Phys. Lett.* **1980**, *76*, 163.
(17) Bergner, A.; Dolg, M.; Küchle, W.; Stoll, H.; Preuss, H. *Mol. Phys.* **1993**, *80*, 1431.
(18) Andzelm, J.; Huzinaga, S.; Klobukowski, M.; Radzio, E.; Sakai, Y.; Tatekawi, H. *Gaussian Basis Sets for Molecular Calculations*; Elsevier: Amsterdam, 1984.
(19) (a) Becke, A. C. *Phys Rev.* **1988**, *A37*, 785. (b) Lee, C.; Yang, W.; Parr, R. G. *Phys. Rev.* **1988**, *B41*, 785. (c) Becke, A. D. *J. Chem. Phys.* **1993**, *98*, 5648. (d) Stevens, D. J.; Devlin, F. J.; Chablowski, C. F.; Frisch, M. J. *J. Phys. Chem.* **1994**, *80*, 11623.
(20) Frisch, M. J.; Trucks, G. W.; Schlegel, H. B.; Gill, P. M. W.; Johnson, B. G.; Robb, M. A.; Cheeseman, J. R.; Keith, T. A.; Petersson, G. A.; Montgomery, J. A.; Raghavachari, K.; Al-Laham, M. A.; Zakrzewski, V. G.; Ortiz, J. V.; Foresman, J. B.; Cioslowski, J.; Stefanov, B. B.; Nanayakkara, A.; Challacombe, M.; Peng, C. Y.; Ayala, P. Y.; Chen, W.; Wong, M. W.; Andres, J. L.; Replogle, E. S.; Gomberts, R.; Martin, R. L.; Fox, D. J.; Binkley, J. S.; Defrees, D. J.; Baker, I.; Stewart, J. J. P.; Head-Gordon, M.; Gonzalez, C.; Pople, J. A. *Gaussian 94*; Gaussian Inc.: Pittsburgh, PA, 1995. Frisch, M. J.; Trucks, G. W.; Schlegel, H. B.; Scuseria, G. E.; Robb, M. A.; Cheeseman, J. R.; Zakrzewski, V. G.; Montgomery, J. A.; Stratmann, R. E.; Burant, J. C.; Dapprich, S.; Milliam, J. M.; Daniels, A. D.; Kudin, K. N.; Strain, M. C.; Farkas, O.; Tomasi, J.; Barone, V.; Cossi, M.; Cammi, R.; Mennucci, B.; Pomelli, C.; Adamo, C.; Clifford, S.; Ochterski, J.; Petersson, G. A.; Ayala, P. Y.; Cui, Q.; Morokuma, K.; Malick, D. K.; Rabuck, A. D.; Raghavachari, K.; Foresman, J. B.; Cioslowski, J.; Ortiz, J. V.; Stefanov, B. B.; Liu, G.; Liashenko, A.; Piskorz, P.; Komaromi, I.; Gomberts, R.; Martin, R. L., Fox, D. J.; Keith, T. A.; Al-Laham, M. A.; Peng, C. Y.; Nanayakkara, A.; Gonzalez, C.; Challacombe, M.; Gill, P. M. W.; Johnson, B. G.; Chen, W.; Wong, M. W.; Andres, J. L.; Head-Gordon, M.; Replogle, E. S.; Pople, J. A. *Gaussian 98* (Revision A.1); Gaussian Inc.: Pittsburgh, PA, 1998.
(21) Dapprich, S.; Frenking, G. *CDA 2.1*; Marburg, 1994. The program is available via anonymous ftp server: ftp.chemie.uni-marburg.de/pub/cda.
(22) (a) Dewar, M. J. S. *Bull. Soc. Chim. Fr.* **1951**, *18*, C79. (b) Chatt, J.; Duncanson, L. A. *J. Chem. Soc.* **1953**, 2929.
(23) (a) Frenking, G.; Pidun, U. *J. Chem. Soc., Dalton Trans.* **1997**, 1653. (b) Pidun, U.; Frenking, G. *J. Organomet. Chem.* **1996**, *525*, 269. (c) Pidun, U.; Frenking, G. *Organometallics* **1995**, *14*, 5325, (d) Vyboishchikov, S. F.; Frenking, G. *Chem. Eur. J.* **1998**, *4*, 1428.
(24) (a) Ehlers, A. W.; Dapprich, S.; Vyboishchikov, S. F.; Frenking, G. *Organometallics* **1996**, *15*, 105. (b) Dapprich, S.; Frenking, G. *Organometallics* **1996**, *15*, 4547. (c) Frenking, G.; Dapprich, S.; Köhler, K. F.; Koch; W.; Collins, J. R. *Mol. Phys.* **1996**, *89*, 1245. (d) Dapprich, S.; Frenking, G. *Angew. Chem.* **1995**, *107*, 383; *Angew. Chem., Int. Ed. Engl.* **1995**, *34*, 354. (e) Fau, S.; Frenking, G. *Mol. Phys.* **1999**, *96*, 519.
(25) Jutzi, P.; Neumann, B.; Reumann, G.; Stammler, H. G. *Organometallics* **1998**, *17*, 1305.
(26) Lewis, K. E.; Golden, D. M.; Smith, G. P. *J. Am. Chem. Soc.* **1984**, *106*, 3905.
(27) (a) Ehlers, A. W.; Baerends, E. J.; Bickelhaupt, F. M.; Radius, U. *Chem. Eur. J.* **1998**, *4*, 210. (b) Radius, U.; Bickelhaupt, F. M.; Ehlers, A. W.; Goldberg, N.; Hoffmann, R. Inorg. *Chem.* **1998**, *37*, 1080. (c) Bickelhaupt, F. M.; Radius, U.; Ehlers, A. W.; Hoffmann, R.; Baerends, E. J. *New J. Chem.* **1998**, 1.

Table 1. Calculated Bond Lengths (Å) and Energies (kcal/mol) of [(CO)$_4$−Fe−ECp] at BP86//II (Experimental Values Are Given in Parentheses)

E	isomer	sym	Fe−E	E−C$_{Cp}$	Fe−CO$_{ax}$	Fe−CO$_{eq}$	∠E−Fe−CO$_{ax}$	∠E−Fe−CO$_{eq}$	ΔE^a	D_e^b	D_o^b
B	ax	C_1	1.962(2.010)[c]	1.830−1.838 (1.811−1.817)[c]	1.788 (1.793)[c]	1.765 (1.774,1786)[c]	179.6	84.7[f]	0.0	77.99	75.02
B	eq	no energy minimum									
Al	ax	C_1	2.242 (2.231)[d]	2.240−2.243 (2.140−2.153)[d]	1.768 (1.796)[d]	1.772 (1.768)[d]	179.6	85.2[f]	0.0	53.12	51.35
Al	eq	C_1	2.233	2.254−2.256	1.778	1.772	79.5[f]	123.8[f]	+0.8	52.36	50.49
Ga	ax	C_1	2.330 (2.273)[e]	2.355−2.356 (2.226)[e]	1.755 (1.781)[e]	1.782 (1.789)[e]	180.0	87.7[f]	0.0	32.89	31.62
Ga	eq	C_1	2.334	2.381−2.379	1.789	1.769	84.8[f]	121.4[f]	+0.5	32.41	31.01
In	ax	C_s	2.465	2.478−2.480	1.752	1.783	180.0	87.8[f]	0.0	33.86	31.69
In	eq	C_s	2.470	2.498−2.501	1.789	1.767	84.9[f]	121.8[f]	+0.6	33.30	32.03
Tl	ax	C_1	2.580	2.432−3.056	1.748	1.789	179.6	88.6[f]	0.0	16.69	15.81
Tl	eq	C_1	2.607	2.508−2.958	1.796	1.765	87.5, 87.9	118.8, 121.0	−0.4	17.11	16.13

[a] Energy difference between axial and equatorial isomers (kcal/mol). [b] Dissociation energy of the Fe−E bond (kcal/mol). [c] Reference 3. [d] Reference 2. [e] Reference 25. [f] Average value of slightly different angles.

analysis of TM group-13 diyl complexes which gives insight into the TM−ER chemical bond. In this paper we report on calculated equilibrium geometries and transition metal−ER (E = B to Tl) bond dissociation energies of the complexes [(CO)$_4$Fe−ECp], [(CO)$_4$Fe−EN(SiH$_3$)$_2$], [(CO)$_5$W−EN(SiH$_3$)$_2$], [(CO)$_4$Fe−EPh], and [TM(ECH$_3$)$_4$] (TM = Ni, Pd, Pt). The calculations have been carried out using gradient-corrected density functional theory (DFT). The analysis of the bonding situation was performed using the CDA[8] and NBO[11] partitioning scheme.

2. Methods

The geometries of the molecules have been optimized using gradient-corrected density functional theory (DFT) with the functionals BP86.[13] The BP86 calculations were performed with our standard basis set II[14] which has small-core effective core potentials (ECP) and (441/2111/N1) valence basis sets (N = 4, 3, 2 for first, second, and third TM row, respectively)[15] for the transition metals in conjunction with all-electron 6-31G(d) basis sets for the main-group elements H, B, C, N, O, Al, Si.[16] ECPs have also been employed for the heavier group-13 elements Ga, In, and Tl, which have (31/31/1) valence basis sets.[17] The d-type polarization functions for these elements were taken from the literature.[18] The TM−E bond energies and vibrational frequencies also have been calculated at BP86/II. All structures reported here are minima on the potential energy surface. Calculations of the complexes TM(ECH$_3$)$_4$ have also been carried out using Becke's three-parameter hybrid method B3LYP,[19] because we encountered convergency problems with BP86 for some molecules. The energy and frequency calculations have been carried out using Gaussian 94 and Gaussian 98.[20] The program CDA 2.1 has been employed for the CDA calculations.[21]

Inspection of the metal−ligand donor−acceptor interactions was performed using the natural bond orbital (NBO)[11] partitioning scheme and the charge-decomposition analysis (CDA).[8] The CDA has been developed as a quantitative expression of the Dewar−Chatt−Duncanson (DCD) model[22] of synergistic metal−ligand bonding, which considers the ligand→metal σ-donation and ligand←metal π-back-donation as the dominant factors for the metal−ligand bond. In the CDA, the wave function of a complex [L$_n$TM−L] is expressed as a linear combination of the fragment molecular orbitals of the ligand L and the remaining metal fragment L$_n$TM. The orbital contributions are divided into four parts: (i) mixing of the occupied σ-type MOs of L and the unoccupied σ-type MOs of L$_n$TM (σ-donation L→TML$_n$); (ii) mixing of the unoccupied π-type MOs of L and the occupied π-type MOs of L$_n$TM (π-back-donation L←TML$_n$); (iii) mixing of the occupied MOs of L and the occupied MOs of L$_n$TM (repulsive polarization L↔TML$_n$); (iv) mixing of the unoccupied MOs of L and the unoccupied MOs of L$_n$TM (rest term Δ). The latter term should not contribute to the electronic structure of the complex. It has been found that the rest term is a sensitive probe if the compound can be classified as a donor−acceptor complex. A significant deviation from $\Delta = 0$ indicates that the bond L$_n$TM−L has the character of a normal covalent bond between two open-shell fragments, rather than a donor−acceptor bond between a Lewis acid and Lewis base.[9,23] All complexes that have been studied in this investigation gave $\Delta = 0$. The CDA method has been proven to be very useful to estimate the relative donor/acceptor strength of a ligand L.[24]

3. Results

The presentation of the results is arranged in the following way. For each class of compounds we give first the calculated geometries and TM−E bond dissociation energies. Then we discuss the analysis of the bonding situation. We focus on the TM←ER σ-donation and the TM→ER π-back-donation, which is estimated in two different ways. One way is by using the CDA method as described in the Methods section. The NBO partitioning scheme is another way to gain information about the TM−ligand donation and back-donation. The TM→ER π-back-donation is taken from the difference in the p(π) population of atom E between the complex [L$_n$TM−ER] and the free ligand ER calculated with the frozen geometry of the complex. This is termed Δq_π(E). The TM←ER σ-donation Δq_σ(E) is then the difference between the change in the total charge Δq(E) caused by the complex formation and Δq_π(E). We also present the changes in the partial charges of the substituents R between the free ligands ER and the complexes [L$_n$TM−ER], which gives information about the intraligand charge exchange. Although any partitioning scheme such as CDA or NBO uses plausible yet arbitrary decisions in order to divide the interatomic charge distribution into atomic spheres, we think that the results of two different methods should give a reasonable estimate of the relative sizes of donation and back-donation.

3.1. [(CO)$_4$Fe−ECp] (E = B to Tl). Table 1 shows the calculated bond lengths and bond angles and the theoretically predicted Fe−E bond dissociation energies of the axial and equatorial isomers of [(CO)$_4$Fe−ECp]. Figure 2 exhibits the optimized structures of the axial and equatorial forms of [(CO)$_4$Fe−GaCp] and [(CO)$_4$Fe−

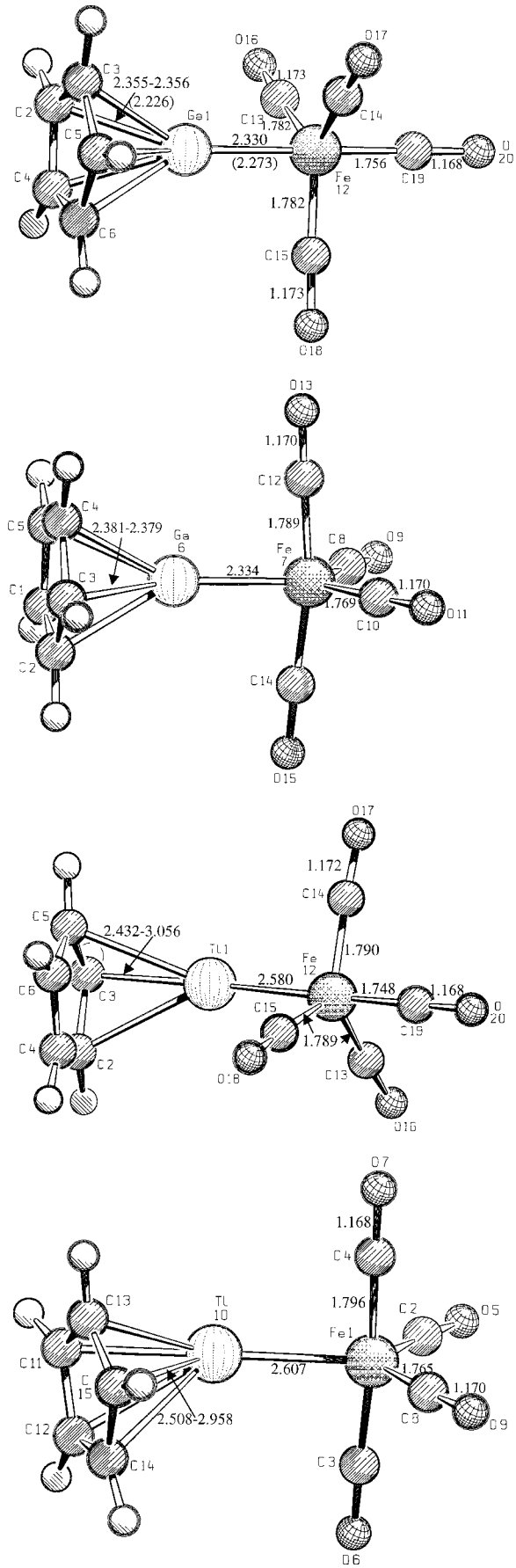

Figure 2. Optimized geometries at BP86/II of the axial and equatorial isomers of [(CO)$_4$Fe−GaCp] and [(CO)$_4$Fe−TlCp]. Bond lengths are given in angstroms. Experimental values are given in parentheses.

TlCp]. The boron, aluminum, and indium homologues have similar structures as the gallium complexes and, thus, are not shown.

The calculations predict that the [(CO)$_4$Fe−ECp] complexes with an axial position of the ECp ligand are slightly more stable than the equatorial forms, except for E = Tl, where the equatorial form is 0.4 kcal/mol lower in energy than the axial form. The energy differences between axial and equatorial isomers are for all complexes very small (<1 kcal/mol). Because of the very small energy difference, we cannot be sure if the theoretical predictions about the most stable form are always correct. However, theory and experiment agree for all molecules where experimental geometries of substituted analogues have been reported.

For the boron complex [(CO)$_4$Fe−BCp] only the axial form was found as an energy minimum. Geometry optimization using the equatorial form as starting geometry led to the axial isomer. The lower energy of the axial form of the Al and Ga complexes is in agreement with experimental results of the complexes [(CO)$_4$Fe−AlCp*] and [(CO)$_4$Fe−GaCp*]. The X-ray structure analyses of the compounds showed that the ECp* ligand is in the axial position.[2,25] The calculated bond lengths of [(CO)$_4$Fe−AlCp] and [(CO)$_4$Fe−GaCp] are in satisfactory agreement with the experimental values of the Cp* analogues (Table 1). The calculated Al−C$_{Cp}$ and Ga−C$_{Cp}$ distances are ∼0.1 Å longer than the experimental values. This can be explained with the use of the Cp model ligand in the calculations, which is a weaker π-donor ligand than Cp*. The Cp ligand in the complexes is bonded in an η^5-mode to the group-13 atoms, except for the thallium compound. The axial and equatorial isomers of [(CO)$_4$Fe−TlCp] have one short Tl−C bond, while two Tl−C bonds have medium length and two Tl−C distances are very long (Table 1). This shows clearly that Tl is a poorer π-acceptor than the lighter group-13 elements. Thallium also has the weakest bond to iron, while boron clearly has the strongest bond. We give for comparison the Fe−CO bond energy of [Fe(CO)$_5$], which is D_e = 48.7 kcal/mol at BP86/II (D_o = 45.9 kcal/mol). The experimental value is D_o = 41 ± 2 kcal/mol.[26] The theoretically predicted Fe−E bond energies at BP86/II might also be slightly too high, but not very much. The calculated values show that the Fe−E bonds are rather strong except for E = Tl. The trend for the Fe−ECp bond strength is E = B > Al > Ga ≈ In > Tl. It will be seen that this ordering holds for the bond dissociation energies of all TM−ER bonds that have been investigated in this study. All complexes show a small umbrella effect where the cis-CO ligands are slightly bend toward ER. The umbrella effect is somewhat stronger in the equatorial isomer of the AlCp complex, where the bond angle <Al−Fe−CO is 79.5° (Table 1). The umbrella effect becomes weaker in the complexes with heavier elements E as ligand atoms. It is interesting to note that the umbrella effect has the same trend as the TM−ECp bond energies.

Table 2 shows the NBO results of the complexes. The Fe atom carries in all complexes a rather large negative charge, while the partial charge at the ligand atoms E is positive and very high for E = Al to Tl. The calculated charge distribution suggests that the Fe−E bond has a strong ionic character. The Fe−E bonds have in all

Table 2. NBO Data of $[(CO)_4-Fe-ECp]$ at BP86/II[a]

E	isomer	q[Fe(CO)$_4$]	q(Fe)	q(E)	q(C$_5$H$_5$)	p_x(E)[b]	p_y(E)[b]	p_z(E)	P(Fe−E)	P(Fe−CO)[c]
				Complexes $[(CO)_4-Fe-ECp]$						
B	ax	−0.51	−0.56	0.32	0.19	0.51	0.51	0.71	0.48	0.70
B	eq	no energy minimum								
Al	ax	−0.67	−0.58	1.18	−0.51	0.29	0.29	0.26	0.48	0.69
Al	eq	−0.60	−0.59	1.12	−0.52	0.33	0.23	0.26	0.44	0.65
Ga	ax	−0.46	−0.51	0.96	−0.50	0.27	0.27	0.21	0.49	0.77
Ga	eq	−0.37	−0.55	0.88	−0.51	0.29	0.22	0.21	0.41	0.69
In	ax	−0.53	−0.49	1.06	−0.53	0.25	0.25	0.19	0.48	0.78
In	eq	−0.44	−0.54	0.98	−0.54	0.20	0.19	0.27	0.40	0.69
Tl	ax	−0.41	−0.45	0.89	−0.48	0.20	0.18	0.14	0.39	0.67
Tl	eq	−0.30	−0.51	0.81	−0.51				0.32	0.73
				Free Ligands ECp[d]						
B	ax			0.05	−0.05	0.31	0.31	0.69		
B	eq	no energy minimum								
Al	ax			0.59	−0.59	0.14	0.14	0.26		
Al	eq			0.59	−0.59	0.14	0.14	0.25		
Ga	ax			0.59	−0.59	0.15	0.15	0.18		
Ga	eq			0.59	−0.59	0.15	0.15	0.17		
In	ax			0.61	−0.61	0.15	0.15	0.18		
In	eq			0.61	−0.61	0.15	0.15	0.17		
Tl	ax			0.64	−0.64	0.16	0.14	0.10		
Tl	eq			0.63	−0.63	0.15	0.16	0.10		

[a] Partial charges q, p-orbital population, Wiberg bond indices P. [b] $p(\pi)$-AO of atom E. [c] CO_{ax} trans to ECp; CO_{eq} in case of the equatorial isomer. [d] Calculated using the frozen geometries in the complexes.

Table 3. NBO and CDA Data of the Changes in the Metal and Ligand Population of $[(CO)_4-Fe-ECp]$ at BP86/II[a]

E	isomer	Δq(E)	Δq_π(E)	Δq_σ(E)	Δq(C$_5$H$_5$)	d(CpE→Fe)	b(CpE←Fe)
B	ax	+0.27	−0.40	+0.67	+0.24	0.598	0.277
B	eq		no energy minimum				
Al	ax	+0.59	−0.30	+0.89	+0.08	0.401	0.188
Al	eq	+0.53	−0.28	+0.81	+0.07	0.364	0.164
Ga	ax	+0.37	−0.24	+0.61	+0.09	0.413	0.039
Ga	eq	+0.29	−0.21	+0.50	+0.08	0.399	0.051
In	ax	+0.45	−0.19	+0.64	+0.06	0.361	0.187
In	eq	+0.35	−0.09	+0.44	+0.07	0.342	0.153
Tl	ax	+0.25	−0.08	+0.33	+0.16	0.238	0.102
Tl	eq	+0.18			+0.12	0.240	0.063

[a] Change in partial charges Δq; difference of the π-population Δq_π; and the σ-charges Δq_σ of the atom E; change in the partial charges Δq(C$_5$H$_5$) of the C$_5$H$_5$ fragments between the complex and the free ligand; positive values indicate that the electronic charge decreases; negative values indicate that the electronic charge increases; charge donation d and back-donation b.

complexes a rather low Wiberg bond order of < 0.5, which is even less than the bond orders of the Fe−CO bonds (Table 2). This is another strong indication that the nature of the Fe−E bond is largely ionic and that the covalent contributions to the binding interactions are less important. Note that the partial charges at atoms E show the rather irregular trend B ≪ Al > Ga < In > Tl. This comes from the trend of the electronegativities and ionization energies of the atoms that do not exhibit a smooth trend along the column of the periodic table of the elements.

Table 3 gives the NBO and CDA results that show the changes that take place in the electronic structure when the Fe−E bond is formed. The population of the degenerate p(π)-AOs at atom E given by the NBO method increases, while the positive atomic charge at E increases in the complexes. Thus, there is a significant reorganization of the σ- and π-charges at atom E, which leads to comparatively small changes in the total charge. The calculated Δq_σ(E) values suggest that there is a substantial σ-donation Fe←ECp, which is clearly higher than the π-back-donation Fe→ECp. The same result is given by the CDA calculations (Table 3). The changes in the partial charge of the Cp ligand are rather small, except for the boron complex. The alteration in the partial charges at boron (+0.27 e) and the Cp substituent (+0.24 e) shows that nearly half of the total charge donation Fe←BCp given by the NBO method comes from the Cp ligand. However, this is a somewhat misleading number, because the actual boron→iron σ-donation is much higher (+0.67 e).

3.2. $[(CO)_4Fe-EN(SiH_3)_2]$ and $[(CO)_5W-EN(SiH_3)_2]$ (E = B to Tl). Table 4 shows the optimized bond lengths and bond angles and the calculated Fe−E bond energies of the iron complexes $[(CO)_4Fe-EN(SiH_3)_2]$. The theoretically predicted interatomic distances and bond energies of the tungsten complexes $[(CO)_5W-EN(SiH_3)_2]$ are shown in Table 5. Figure 3 displays the calculated structures of the compounds with E = Ga. The B, Al, In, and Tl complexes have a similar structure and therefore are not shown here.

The only complex of the series for which an experimental geometry of a related compound is available is $[(CO)_5W-BN(SiH_3)_2]$.[4] Table 4 shows that the agreement between theory and experiment is quite good. The calculated W−E bond is slightly too short and the E−Si bond is too long by 0.044 Å, which may partly be due to the model substituent that is used in the calculation (SiH_3 instead of $SiMe_3$). The theoretically predicted relative energies of the axial and equatorial isomers of

Table 4. Calculated Bond Lengths (Å) and Energies (kcal/mol) of $[(CO)_4-Fe-EN(SiH_3)_2]$

E	isomer	sym	Fe−E	E−N	Fe−CO_{ax}	Fe−CO_{eq}	∠E−Fe−CO_{ax}	∠E−Fe−CO_{eq}	ΔE^a	D_e^b	D_o^b
B	ax	no energy minimum									
B	eq	C_1	1.818	1.382	1.777	1.790	77.6	125.7	−	85.83	83.09
Al	ax	C_s	2.211	1.802	1.771	1.777	177.4	86.1[c]	0.0	51.84	50.23
Al	eq	C_s	2.199	1.810	1.782	1.777	80.2	124.2	−1.1	52.98	51.18
Ga	ax	C_s	2.274	1.876	1.764	1.783	178.7	87.9[c]	0.0	39.68	38.20
Ga	eq	C_s	2.273	1.887	1.791	1.774	84.5	122.7	+0.2	39.53	37.87
In	ax	C_s	2.420	2.023	1.758	1.783	179.1	88.0[c]	0.0	38.92	37.49
In	eq	C_s	2.422	2.034	1.791	1.770	84.5	123.5	+0.7	38.20	36.65
Tl	ax	C_s	2.530	2.123	1.752	1.789	179.5	89.2[c]	0.0	25.35	24.17
Tl	eq	C_s	2.540	2.144	1.796	1.769	87.5	121.4	+0.4	24.95	22.47

[a] Energy difference between axial and equatorial isomers [kcal/mol]. [b] Dissociation energy of the Fe−E bond [kcal/mol]. [c] Average value of slightly different angles.

Table 5. Calculated Bond Lengths (Å) and Dissociation Energies (kcal/mol) of $[(CO)_5-W-EN(SiH_3)_2]$ (Experimental Values Are Given in Parentheses)

E	sym	W−E	E−N	W−CO_{trans}	W−CO_{cis}	∠E−W−CO_{trans}	∠E−W−CO_{cis}[a]	D_e^b	D_o^b
B	C_2	2.125 (2.152)[c]	1.383 (1.339)[c]	2.078	2.059	180.0	88.3	75.08	73.41
Al	C_{2v}	2.530	1.816	2.028	2.057	180.0	89.1	44.40	43.48
Ga	C_{2v}	2.551	1.893	2.022	2.058	180.0	89.6	36.69	35.79
In	C_{2v}	2.679	2.033	2.015	2.057	180.0	89.9	36.46	35.57
Tl	C_{2v}	2.792	2.134	2.004	2.057	180.0	89.7	25.24	24.52

[a] Average value of slightly different angles. [b] Dissociation energy of the W−E bond [kcal/mol]. [c] Reference 4.

$[(CO)_4Fe-EN(SiH_3)_2]$ are quite interesting, because they are partly different from the results for the Cp complexes reported above. In particular the results for the boron complex are intriguing, since only the equatorial isomer was found to be a minimum on the potential energy surface. This is opposite the Cp complex, where only the axial isomer is a stable species (Table 1). The compound $[(CO)_4Fe-BN(SiMe_3)_2]$ has been synthesized, but the authors did not report the structure of the complex.[4] A recent theoretical study of the parent compound $[(CO)_4Fe-ENH_2]$ at the DFT level predicted that the axial isomer is a minimum on the potential energy surface and that it is lower in energy than the equatorial form.[27] The axial isomer encounters steric interactions between the NR_2 ligand and three equatorial CO groups (bond angle $NR_2-Fe-CO_{eq}$ ~90°), while the equatorial isomer has steric repulsion between NR_2 and only two axial CO ligands (bond angle $NR_2-Fe-CO_{ax}$ ~90°). The other two equatorial CO ligands are bent away from NR_2 (Figure 3). However, steric arguments are not the reason only the equatorial isomer of $[(CO)_4Fe-EN(SiH_3)_2]$ was found as a minimum on the potential energy surface. Calculations of the parent molecule $[(CO)_4Fe-ENH_2]$ at BP86/II predicted that the equatorial isomer is 2.08 kcal/mol lower in energy than the axial form, which is a transition state ($i = 1$). We do not know the reason for the difference between our results and those reported in ref 27. For the aluminum complex $[(CO)_4Fe-AlN(SiH_3)_2]$ both isomers were obtained, but the equatorial form is lower in energy than the axial form. Only for the heavier analogues E = Ga, In, and Tl, which have longer Fe−E and E−N bonds, are the axial forms more stable than the equatorial form (Table 3). The calculations predict that the complex $[(CO)_4Fe-BN(SiMe_3)_2]$, which was synthesized by Braunschweig, should have the $BN(SiMe_3)_2$ ligand in the equatorial position, because it is even bulkier than $BN(SiH_3)_2$.[4]

Both sets of complexes $[(CO)_4Fe-EN(SiH_3)_2]$ and $[(CO)_5W-EN(SiH_3)_2]$ exhibit a small umbrella effect where the cis CO ligand is bent toward ER. The bending angle becomes smaller when E becomes heavier. A comparison of the calculated Fe−E bond distances of $[(CO)_4Fe-EN(SiH_3)_2]$ with those of $[(CO)_4Fe-ECp]$ shows that the former bonds are always shorter than the latter (Tables 1 and 4). A particularly noteworthy bond length is the Fe−B bond distance in $[(CO)_4Fe-BN(SiH_3)_2]$, which is substantially shorter (1.818 Å) than in $[(CO)_4Fe-BCp]$ (1.962 Å). The differences in the Fe−E bond lengths between $[(CO)_4Fe-EN(SiH_3)_2]$ and $[(CO)_4Fe-ECp]$ do not correlate with the differences in the bond dissociation energies. Tables 1 and 4 show that only the boron compound of the former series is more strongly bonded than the BCp complex. The aluminum complexes of the two series have nearly the same bond energy, while the ECp complexes of the heavier analogues, E = Ga, In, Tl, are clearly more strongly bonded than the respective $EN(SiH_3)_2$ complexes. The $[(CO)_4Fe-EN(SiH_3)_2]$ compounds have generally stronger TM−E bonds than the $[(CO)_5W-EN(SiH_3)_2]$ compounds (Tables 4 and 5). The difference in the bond energy becomes smaller for the heavier group-13 elements and finally vanishes for the thallium complexes, where the Fe−Tl and W−Tl bond strengths are nearly the same. For both series of $[TM-EN(SiH_3)_2]$, however, the trend of the TM−E bond energies is the same as that for the TM−ECp complexes, i.e., B > Al > Ga ≈ In > Tl.

Tables 6 and 7 show the results of the NBO partitioning scheme for the aminoborylene complexes. The Fe−E and W−E bonds have a strong ionic character. This becomes obvious from the calculated charge distribution, which gives large positive charges for the group-13 elements E and large negative charges for the transition metals, and from the Wiberg bond indices P(TM−E), which are in most cases lower than the P(TM−CO) values. The largest covalent contributions are found for the TM−boron bonds, which arise from the comparatively high TM→B π-back-donation (see below). We want to point out that the population of the nitrogen p(π)-AO changes little when the $N(SiH_3)_2$ ligand becomes

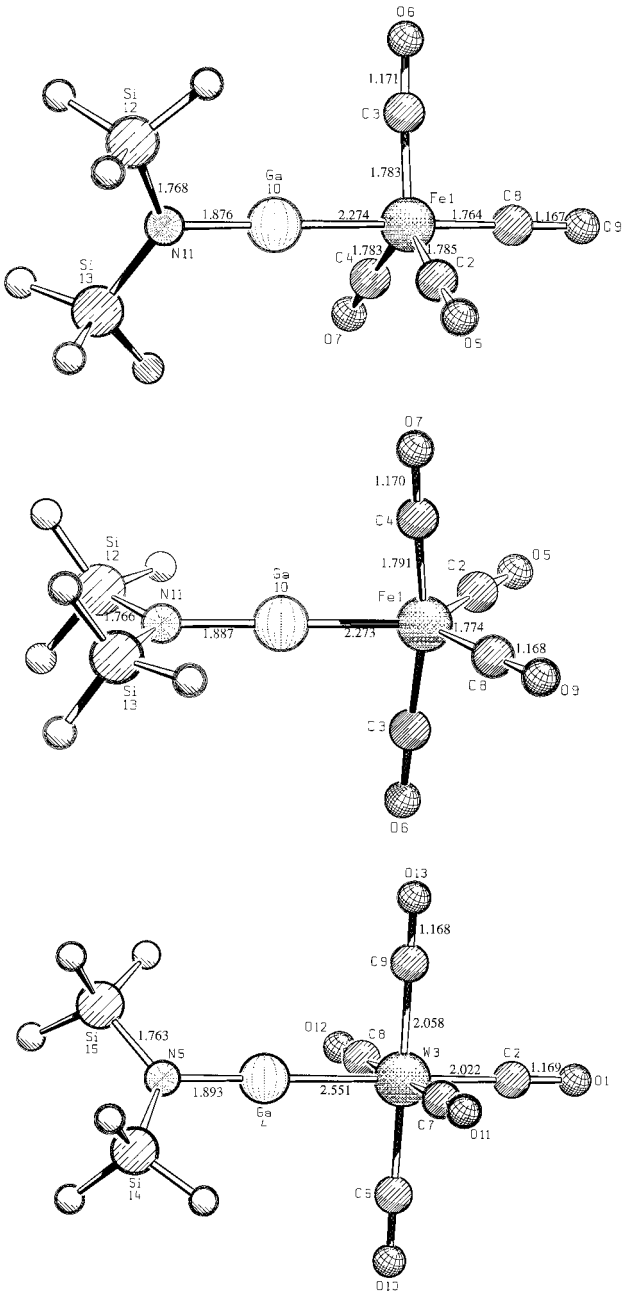

Figure 3. Optimized geometries at BP86/II of the axial and equatorial isomers of $[(CO)_4Fe-GaN(SiH_3)_2]$ and $[(CO)_5W-GaN(SiH_3)_2]$. Bond lengths are given in angstroms.

bonded to the metal. This means that the TM→EN-$(SiH_3)_2$ π-back-donation has only a small influence on the E←$N(SiH_3)_2$ π-donation.

The difference in the population of the in-plane and out-of-plan p(π)-AO of E (Figure 4) between the free ligand and the complex gives insight into the π-donation of the amino group and the iron atom toward E. Tables 6 and 7 show that the in-plane p(π)-AO of E is nearly empty in the free ligand, but it becomes equally or even higher occupied than the out-of-plane p(π) in the complex. Both p(π)-AOs of E become more highly populated in the complexes, which shows that the Fe→E π-back-donation is quite effective. Tables 8 and 9 show the differences in the charge distribution of the fragments when the TM−E bond is formed. Note that the change in the partial charge at the boron atom of $[(CO)_4Fe-BN(SiH_3)_2]$ (Δq(E) = +0.08 e) is smaller than the alteration in the partial charge of the aminosilyl group ($\Delta q(N(SiH_3)_2$ = +0.23 e). And yet, the changes in the electronic structure at boron are much higher than at the aminosilyl group, because there are large changes in the σ- and π-charges at the boron atom of $[(CO)_4Fe-BN(SiH_3)_2]$ Δq_σ(B) = +0.68 e and Δq_π(B) = −0.60 e (Table 8). The same result is given by the charge decomposition analysis. Large changes in the σ/π-charges are also predicted for $[(CO)_5W-BN(SiH_3)_2]$ and for the heavier analogues $[(CO)_4Fe-EN(SiH_3)_2]$ and $(CO)_5W-EN(SiH_3)_2$ (Tables 8 and 9). The NBO analysis suggests that the TM←$EN(SiH_3)_2$ σ-donation is very high for all elements E and that the largest σ-donation is found for E = Al. The CDA results indicate that the σ-donation becomes less for the heavier group-13 elements. Both methods agree, however, that the σ-donation is larger than the π-back-donation.

It is interesting to compare the results of the bonding analysis of $[(CO)_4Fe-BCp]$ with $[(CO)_4Fe-BN(SiH_3)_2]$, because these molecules are models for the first borylene complexes that have been synthesized.[3,4] The results of the NBO and CDA methods show that the Fe→B π-back-donation in the Cp-substituted borylene complex is smaller than in the aminosilyl-subsituted borylene (Tables 3 and 8). However, the results of the bonding analysis do not suggest a fundamental difference in the bonding situation between the two compounds, which is in both molecules mainly determined by charge interactions.

3.3. $[(CO)_4Fe-EPh]$ (E = B to Tl). The TM complexes $[(CO)_nTM-ER]$ discussed so far had substituents R at the group-13 atom which are strong π-donors. The phenyl group in $[(CO)_4Fe-EPh]$ should provide only weak π-stabilization of the out-of-plane p(π) of E through conjugation with the π-electron of the phenyl ring, and the in-plane p(π)-AO should not receive any stabilization by the phenyl ring (Figure 5). Electronic stabilization of the electron-deficient group-13 atoms should mainly come from Fe→E π-back-donation.

Figure 6 shows the optimized geometries of the axial and equatorial isomers of $[(CO)_4Fe-GaPh]$. The other group-13 homologues have a similar structure and are therefore not shown. Table 10 shows the most important calculated bond lengths and bond angles. The experimental values for the complex $[(CO)_4Fe-EPh^*]$ are also given.[5] They are in good agreement with the theoretical results.

The calculated Fe−E interatomic distances of the complexes $[(CO)_4Fe-EPh]$ are clearly shorter than the bond lengths of the $[(CO)_4Fe-ECp]$ and $[(CO)_4Fe-EN(SiH_3)_2]$ molecules (Tables 1 and 4). The shorter bond lengths support the assumption that the Fe→E π-back-donation in the phenyl-substituted complexes is larger than in the cyclopentadienyl- and amino-substituted compounds. The calculated Fe−EPh bond dissociation energies are also significantly higher than the Fe−ECp and $[Fe-EN(SiH_3)_2]$ compounds. Even the thallium complex $[(CO)_4Fe-TlPh]$ has a rather high bond energy D_e = 42.5 kcal/mol and, thus, may be a promising target for experimental studies. The isomers with axial EPh ligands are slightly lower in energy than the equatorial

Table 6. NBO Data of $[(CO)_4-Fe-EN(SiH_3)_2]$ at BP86/II[a]

E	isomer	q[Fe(CO)$_4$]	q(Fe)	q(E)	q(N)	p_x(E)[b]	p_y(E)[c]	p_z(E)	p_π(N)[f]	P(Fe−E)	P(Fe−CO)[d]
					Complexes $[(CO)_4-Fe-EN(SiH_3)_2]$						
B	*ax*	no energy minimum									
B	*eq*	−0.31	−0.58	0.59	−1.49	0.39	0.48	0.61	1.67	0.65	0.62
Al	ax	−0.64	−0.60	1.31	−1.79	0.26	0.23	0.20	1.79	0.53	0.67
Al	eq	−0.57	−0.63	1.23	−1.79	0.20	0.30	0.21	1.78	0.51	0.63
Ga	ax	−0.53	−0.56	1.14	−1.73	0.24	0.20	0.19	1.79	0.53	0.71
Ga	eq	−0.43	−0.60	1.06	−1.73	0.17	0.25	0.20	1.78	0.50	0.65
In	ax	−0.57	−0.53	1.21	−1.71	0.21	0.17	0.16	1.79	0.50	0.73
In	eq	−0.48	−0.58	1.13	−1.71	0.15	0.23	0.17	1.78	0.47	0.65
Tl	ax	−0.46	−0.48	1.07	−1.66	0.18	0.14	0.13	1.79	0.44	0.79
Tl	eq	−0.36	−0.54	1.00	−1.67	0.13	0.17	0.13	1.78	0.40	0.69
					Free Ligands $EN(SiH_3)_2$[e]						
B	ax	no energy minimum									
B	eq			0.51	−1.62	0.21	0.06	0.57	1.72		
Al	ax			0.79	−1.83	0.11	0.02	0.23	1.77		
Al	eq			0.79	−1.83	0.11	0.02	0.23	1.77		
Ga	ax			0.76	−1.78	0.11	0.02	0.23	1.77		
Ga	eq			0.77	−1.78	0.11	0.02	0.23	1.77		
In	ax			0.78	−1.75	0.10	0.01	0.22	1.76		
In	eq			0.78	−1.75	0.10	0.01	0.22	1.76		
Tl	ax			0.79	−1.72	0.10	0.01	0.20	1.76		
Tl	eq			0.77	−1.72	0.10	0.01	0.19	1.77		

[a] Partial charges q, p-orbital population and Wiberg bond indices P. [b] $p(\pi)$-AO of atom E which is perpendicular to the Si−N−Si plane. [c] $p(\pi)$-AO of atom E which is in the Si−N−Si plane. [d] CO_{ax} trans to $EN(SiH_3)_2$; CO_{eq} in case of the equatorial isomer. [e] Calculated using the frozen geometries in the complexes. [f] Population of the nitrogen lone-pair orbital.

Table 7. NBO Data of $[(CO)_5-W-EN(SiH_3)_2]$ at BP86/II[a]

E	q[W(CO)$_5$]	q(W)	q(E)	q(N)	p_x(E)[b]	p_y(E)[c]	p_z(E)	p_π(N)[f]	P(W−E)	P(W−CO)[d]
				Complex $[(CO)_5$-W−$EN(SiH_3)_2]$						
B	−0.36	−0.87	0.69	−1.50	0.30	0.31	0.66	1.78	0.82	0.75
Al	−0.61	−0.99	1.30	−1.81	0.17	0.11	0.23	1.78	0.56	0.84
Ga	−0.54	−0.96	1.20	−1.75	0.16	0.10	0.21	1.78	0.53	0.87
In	−0.60	−0.93	1.27	−1.73	0.14	0.08	0.17	1.78	0.50	0.89
Tl	−0.50	−0.86	1.15	−1.68	0.12	0.07	0.14	1.78	0.44	0.94
				Free Ligand $EN(SiH_3)_2$[e]						
B			0.51	−1.62	0.21	0.06	0.57	1.72		
Al			0.79	−1.83	0.11	0.02	0.22	1.77		
Ga			0.77	−1.78	0.11	0.02	0.23	1.77		
In			0.78	−1.75	0.10	0.01	0.22	1.76		
Tl			0.77	−1.72	0.10	0.01	0.19	1.76		

[a] Partial charges q, p-orbital population and Wiberg bond indices P. [b] $p(\pi)$-AO of atom E which is perpendicular to the Si−N−Si plane. [c] $p(\pi)$-AO of atom E which is in the Si−N−Si plane. [d] CO_{ax} trans to $EN(SiH_3)_2$; CO_{eq} in case of the equatorial isomer. [e] Calculated using the frozen geometries in the complexes. [f] Population of the nitrogen lone-pair orbital.

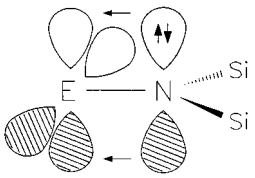

Figure 4. Schematic representation of the π-bonding interactions in $E-NH_2$.

forms, except for the aluminum compound, where the axial and equatorial isomers are nearly degenerate (Table 10). The ordering of the bond strength is the same as for the other compounds, i.e., B > Al > Ga ≈ In > Tl. The complexes with EPh ligands show a similar umbrella effect as the other compounds with ER ligands.

Table 11 shows the results of the NBO analysis. Like in the other complexes with TM−E bonds, there is strong Coulombic attraction between the positively charged atom E and the negatively charged iron atom (Table 11). The p(π)-AOs of E, which are nearly empty in the free ligands EPh, become significantly populated in the complexes. Please note that, in the axial isomers of the complexes, the out-of-plane p(π)-AO of E carries more electronic charge than the in-plane p(π)-AO, while the equatorial isomers show the opposite order. The covalent contributions to the Fe−E bonding remain small, however. The Wiberg bond indices for the Fe−EPh bonds are < 1 for all ligand atoms E, and only the Fe−BPh bond order is slightly higher than the Fe−CO bond index.

Table 12 gives the changes in the charge distribution of the fragments after the Fe−E bond is formed. The calculated data support the conclusion that the Fe→EPh π-back-donation in $[(CO)_4Fe-EPh]$ is stronger than in the other group-13 complexes. This is revealed by the NBO data for Δq_π(E) and by the CDA results for the ratio of Fe←EPh donation to Fe→EPh π-back-donation. We want to point out, however, that the calculated Fe→EPh π-back-donation is only slightly higher than the Fe→$EN(SiH_3)_2$ π-back-donation (Table 8), although the p(π)-AOs of E in free EPh are nearly empty (Table 11), while they are partly occupied in $EN(SiH_3)_2$ (Table 6). The Fe←EPh σ-donation is also the largest among the investigated group-13 complexes. Part of the Fe←EPh σ-donation comes from the phenyl group, which donates between 0.15 and 0.31 e toward E (Table 12).

Table 8. NBO and CDA Data of the Changes in the Metal and Ligand Population of $[(CO)_4$-Fe−$EN(SiH_3)_2]$ at BP86/II[a]

E	isomer	Δq(E)	Δq_π(E)	Δq_σ(E)	Δq_π(N)	Δq(N(SiH$_3$)$_2$)	d(E→Fe)	b(E←Fe)
B	ax		no energy minimum					
B	eq	+0.08	−0.60	+0.68	+0.05	+0.23	0.583	0.476
Al	ax	+0.52	−0.36	+0.88	−0.02	+0.12	0.419	0.237
Al	eq	+0.44	−0.37	+0.81	−0.01	+0.13	0.368	0.208
Ga	ax	+0.38	−0.31	+0.69	−0.02	+0.15	0.393	0.128
Ga	eq	+0.29	−0.29	+0.58	−0.01	+0.14	0.356	0.145
In	ax	+0.43	−0.27	+0.70	−0.03	+0.14	0.214	0.165
In	eq	+0.35	−0.27	+0.62	−0.02	+0.13	0.211	0.175
Tl	ax	+0.28	−0.21	+0.49	−0.03	+0.18	0.243	0.079
Tl	eq	+0.23	−0.19	+0.42	−0.01	+0.13	0.222	0.061

[a] Change in partial charges Δq; difference of the π-population Δq_π; and the σ-charges Δq_σ of the atom E; change in the partial charges Δq(N(SiH$_3$)$_2$) of the N(SiH$_3$)$_2$ fragments between the complex and the free ligand; positive values indicate that the electronic charge decreases; negative values indicate that the electronic charge increases; charge donation d and back-donation b.

Table 9. NBO and CDA Data of the Changes in the Metal and Ligand Population of $[(CO)_5$−W−$EN(SiH_3)_2]$ at BP86/II[a]

E	Δq(E)	Δq_π(E)	Δq_σ(E)	Δq_π(N)	Δq(N(SiH$_3$)$_2$)	d(E→W)	b(E←W)
B	+0.18	−0.34	+0.52	−0.06	+0.18	0.750	0.329
Al	+0.51	−0.15	+0.66	−0.01	+0.10	0.566	0.287
Ga	+0.43	−0.13	+0.56	−0.01	+0.10	0.509	0.258
In	+0.49	−0.11	+0.60	−0.02	+0.11	0.309	0.186
Tl	+0.38	−0.08	+0.46	−0.02	+0.12	0.432	0.155

[a] Change in partial charges Δq; difference of the π-population Δq_π; and the σ-charges Δq_σ of the atom E; change in the partial charges Δq(N(SiH$_3$)$_2$) of the N(SiH$_3$)$_2$ fragments between the complex and the free ligand; positive values indicate that the electronic charge decreases; negative values indicate that the electronic charge increases; charge donation d and back-donation b.

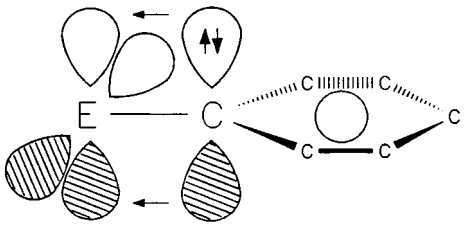

Figure 5. Schematic representation of the π-bonding interactions in E−Ph.

3.4. $[TM(ECH_3)_4]$ (TM = Ni, Pd, Pt; E = B to Tl). The compounds $[Ni(ECH_3)_4]$, $[Pd(ECH_3)_4]$, and $[Pt(ECH_3)_4]$ are different from the other complexes with group-13 ligands that have been discussed so far, because they are *homoleptic* complexes of *late* transition metals. Two related nickel compounds with larger substituents, [Ni(Ga−C(SiMe$_3$)$_3$)$_4$] and [Ni(In−C(SiMe$_3$)$_3$)$_4$], have recently been synthesized.[6,7] The BP86/II calculations of $[TM(ECH_3)_4]$ encountered severe convergence problems, which could not be resolved in a few cases. We decided to carry out calculations at B3LYP/II, which did not suffer from the same SCF problems. We report the results for $[TM(ECH_3)_4]$ at both levels of theory, which makes it also possible to see the alterations of the results when different methods are used.

Table 13 shows that the optimized Ni−E and E−C bond lengths of the model complexes are in very good agreement with the results of the X-ray structure analyses. The differences between BP86/II and B3LYP/II for the calculated bond lengths are rather small. Figure 7 shows the optimized geometry of $[Ni(GaCH_3)_4]$. The other $[TM(ECH_3)_4]$ complexes have a similar structure and are therefore not shown.

The calculations show that the first TM−ECH_3 bond dissociation energies are rather high. The theoretical bond energies at B3LYP/II are always 5−8 kcal/mol higher than the BP86/II values (Table 13). The strength of the TM−ECH_3 bonds becomes obvious by comparison

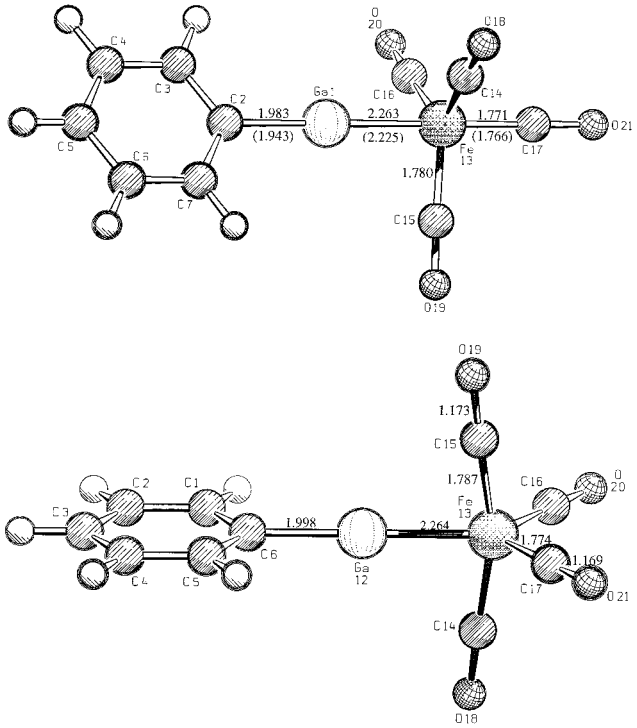

Figure 6. Optimized geometries at BP86/II of the axial and equatorial isomers of $[(CO)_4Fe-GaPh]$. Bond lengths are given in angstroms. Experimental values are given in parentheses.

with the TM−CO bonds in $[TM(CO)_4]$, which have much lower bond energies. The calculated first TM−CO bond dissociation energies at the CCSD(T)/II level of theory are D_o = 22.3 kcal/mol for $[Ni(CO)_4]$, D_o = 7.5 kcal/mol for $[Pd(CO)_4]$, and D_o = 10.9 kcal/mol for $[Pt(CO)_4]$.[28]

(28) (a) Ehlers, A. W.; Frenking, G. *Organometallics* **1995**, *14*, 423. (b) Ehlers, A. W.; Dapprich, S.; Vyboishchikov, S. F.; Frenking, G. *Organometallics* **1996**, *15*, 105.

Table 10. Calculated Bond Lengths (Å) and Energies (kcal/mol) of [(CO)$_4$−Fe−EPh] at BP86/II (Experimental Values Are Given in Parentheses)

E	isomer	sym	Fe−E	E−C$_{Ph}$	Fe−CO$_{ax}$	Fe−CO$_{eq}$	∠E−Fe−CO$_{ax}$	∠E−Fe−CO$_{eq}$	ΔE[a]	D_e[b]	D_o[b]
B	ax	C_s	1.800	1.515	1.824	1.774	179.3	85.1[d]	0.0	102.77	99.79
Al	ax	C_s	2.206	1.952	1.777	1.775	179.4	85.2[d]	0.0	63.51	61.54
Al	eq	C_{2v}	2.199	1.955	1.782	1.777	78.4	125.4	−0.1	63.60	61.53
Ga	ax	C_s	2.263 (2.225)[c]	1.983 (1.943)[c]	1.771 (1.766)[c]	1.780 (1.764)[c]	179.6	86.8[d]	0.0	55.03	53.16
Ga	eq	C_1	2.264	1.988	1.787	1.774	81.9	124.6	+1.7	53.33	51.36
In	ax	C_s	2.411	2.134	1.764	1.780	179.7	86.9[d]	0.0	53.24	51.48
In	eq	C_1	2.414	2.141	1.787	1.770	82.0	124.9	+2.0	51.29	49.43
Tl	ax	C_s	2.506	2.216	1.760	1.784	179.8	88.0[d]	0.0	42.52	40.95
Tl	eq	C_1	2.515	2.229	1.790	1.768	84.7	123.7[d]	+2.5	40.04	38.36

[a] Energy difference between axial and equatorial isomers (kcal/mol). [b] Dissociation energy of the Fe−E bond (kcal/mol). [c] Reference 5. [d] Average value of slightly different angles.

Table 11. NBO Data of [(CO)$_4$−Fe−EPh] at BP86/II[a]

E	isomer	q[Fe(CO)$_4$]	q(Fe)	q(E)	q(C$_6$H$_5$)	p_x(E)[b]	p$_y$(E)[c]	p_z(E)	p_π(C$_6$H$_5$)	P(Fe−E)	P(Fe−CO)[d]
					Complexes [(CO)$_4$−Fe−EPh]						
B	ax	−0.36	−0.59	0.65	−0.29	0.41	0.34	0.65	5.88	0.76	0.57
B	eq	−0.39	−0.91	0.66	−0.27	0.31	0.41	0.66	5.84	0.64	0.53
Al	ax	−0.73	−0.60	1.27	−0.54	0.23	0.20	0.24	5.93	0.51	0.65
Al	eq	−0.66	−0.62	1.20	−0.54	0.15	0.30	0.27	5.90	0.50	0.63
Ga	ax	−0.63	−0.56	1.12	−0.49	0.21	0.18	0.24	5.94	0.52	0.68
Ga	eq	−0.54	−0.59	1.05	−0.51	0.13	0.27	0.26	5.94	0.51	0.64
In	ax	−0.67	−0.53	1.16	−0.49	0.18	0.16	0.23	5.95	0.49	0.70
In	eq	−0.58	−0.56	1.08	−0.50	0.11	0.26	0.25	5.90	0.48	0.66
Tl	ax	−0.60	−0.50	1.04	−0.44	0.15	0.14	0.19	5.96	0.44	0.74
Tl	eq	−0.54	−0.59	0.98	−0.44	0.10	0.19	0.21	6.03	0.42	0.66
					Free Ligands EPh[e]						
B	ax			0.45	−0.45	0.11	0.01	0.69	5.85		
B	eq			0.45	−0.45	0.11	0.01	0.69	5.87		
Al	ax			0.73	−0.73	0.05	0.00	0.34	5.93		
Al	eq			0.73	−0.73	0.05	0.00	0.34	5.94		
Ga	ax			0.70	−0.70	0.05	0.00	0.36	5.95		
Ga	eq			0.70	−0.70	0.05	0.00	0.36	5.94		
In	ax			0.70	−0.70	0.05	0.00	0.36	5.95		
In	eq			0.70	−0.70	0.06	0.00	0.35	5.94		
Tl	ax			0.68	−0.68	0.04	0.00	0.36	5.95		
Tl	eq			0.68	−0.68	0.04	0.00	0.35	5.96		

[a] Partial charges q, p-orbital population and Wiberg bond indices P. [b] $p(\pi)$-AO of atom E which is perpendicular to the phenyl plane. [c] $p(\pi)$-AO of atom E which is in the phenyl plane. [d] CO$_{ax}$ trans to EPh; CO$_{eq}$ in case of the equatorial isomer. [e] Calculated using the frozen geometries in the complexes.

Table 12. NBO and CDA Data of the Changes in the Metal and Ligand Population of [(CO)$_4$−Fe−EPh] at BP86/II[a]

E	isomer	Δq(E)	Δq_π(E)	Δq_σ(E)	Δq(C$_6$H$_5$)	Δq_π(C$_6$H$_5$)	Δq_σ(C$_6$H$_5$)	d(PhE→Fe)	b(PhE←Fe)
				Complexes [(CO)$_4$−Fe−EPh]					
B	ax	+0.20	−0.63	+0.83	+0.16	−0.03	+0.19	0.516	0.473
B	eq	+0.21	−0.60	+0.81	+0.18	+0.03	+0.15	0.453	0.526
Al	ax	+0.54	−0.38	+0.92	+0.19	+0.00	+0.19	0.453	0.345
Al	eq	+0.47	−0.40	+0.87	+0.19	+0.04	+0.15	0.399	0.335
Ga	ax	+0.42	−0.34	+0.76	+0.21	+0.01	+0.20	0.383	0.264
Ga	eq	+0.35	−0.35	+0.70	+0.19	+0.00	+0.19	0.343	0.283
In	ax	+0.46	−0.29	+0.75	+0.21	+0.00	+0.21	0.388	0.277
In	eq	+0.38	−0.31	+0.69	+0.20	+0.04	+0.16	0.333	0.277
Tl	ax	+0.36	−0.25	+0.61	+0.24	−0.01	+0.25	0.273	0.180
Tl	eq	+0.30	−0.25	+0.55	+0.24	−0.07	+0.31	0.236	0.161

[a] Change in partial charges Δq; difference of the π-population Δq_π; and the σ-charges Δq_σ of the atom E; change in the partial charges Δq(C$_6$H$_5$) of the C$_6$H$_5$ fragments between the complex and the free ligand; positive values indicate that the electronic charge decreases; negative values indicate that the electronic charge increases; charge donation d and back-donation b.

The trend of the TM−ECH$_3$ bond energies shows for the transition metals the order Ni ≈ Pt > Pd, while for the group-13 elements the same trend as for the other complexes is found, B > Al > Ga ≈ In > Tl.

The results of the NBO partitioning scheme are shown in Table 14. The BP86 and B3LYP values are not very different from each other. The p(π)-orbitals of the atoms E, which are nearly empty in the free ligand ECH$_3$, become significantly populated in the complexes. This is a strong indication that there is substantial TM→ECH$_3$ π-back-donation in the molecules. The NBO data suggest that the TM→ECH$_3$ π-back-donation is in some complexes even larger than the TM←ECH$_3$ σ-donation. This can be taken from Table 15, which gives the changes in the charge distribution caused by the TM−E bond formation. The CDA results support the picture of strong TM→ECH$_3$ π-back-donation, although the TM←ECH$_3$ σ-donation is still larger. However, the

Table 13. Calculated Bond Lengths (Å) and Energies (kcal/mol) of [TM(ECH$_3$)$_4$] at BP86/II and B3LYP/II (Experimental Values Are Given in Parentheses)

		TM−E		E−C		D_e[a]		D_o[a]	
E	sym	BP86	B3LYP	BP86	B3LYP	BP86	B3LYP	BP86[d]	B3LYP
				Complexes [Ni(ECH$_3$)$_4$]					
B	T_d	1.771	1.764	1.553	1.548	91.36	83.80	87.26	79.70
Al	T_d	2.153	2.142	1.995	1.987	61.58	55.64	59.18	53.24
Ga	T_d	2.214	2.210 (2.170)[b]	2.047	2.037 (2.014)[b]	49.62	43.15	47.13	40.66
In	T_d	2.347	2.341 (2.310)[c]	2.190	2.182 (2.195)[c]	51.07	45.44	49.07	43.44
Tl	T_d	2.451	2.452	2.291	2.281	*e*	28.39	*e*	27.00
				Complexes [Pd(ECH$_3$)$_4$]					
B	T_d	1.923	1.923	1.552	1.547	76.19	67.46	72.49	63.76
Al	T_d	2.295	2.295	1.994	1.987	52.86	46.02	50.46	43.62
Ga	T_d	2.355	2.362	2.051	2.040	40.34	33.43	38.24	31.33
In	T_d	2.466	2.468	2.192	2.185	43.71	37.42	41.70	35.41
Tl	T_d	2.603	2.622	2.307	2.293	26.81	19.88	25.40	18.47
				Complexes [Pt(ECH$_3$)$_4$]					
B	T_d	1.931	1.928	1.551	1.546	89.34	82.68	85.64	78.98
Al	T_d	2.302	2.298	1.993	1.983	62.80	57.32	60.31	54.83
Ga	T_d	2.347	2.345	2.040	2.028	48.89	43.34	46.70	41.15
In	T_d	2.467	2.464	2.180	2.171	51.85	46.79	49.85	44.79
Tl	T_d	2.576	2.578	2.286	2.272	32.07	26.20	28.58	24.71

[a] First dissociation energy of TM−E bond (kcal/mol). [b] Reference 7. [c] Reference 6. [d] Calculated with ZPE corrections from B3LYP/II. [e] No SCF convergence.

Table 14. NBO Data of [TM(ECH$_3$)$_4$] at BP86/II and B3LYP/II[a]

	q[TM(ER)$_3$]		q(TM)		q(E)		q(CH$_3$)		p_x(E)[b]		p_y(E)		p_z(E)		P(TM−E)	
E	BP86	B3LYP	BP86	B3LYP	BP86	B3LYP	BP86	B3LYP	BP86	B3LYP	BP86	B3LYP	BP86	B3LYP	BP86	B3LYP
							Complexes [Ni(ECH$_3$)$_4$]									
B	*d*	0.04	*d*	0.16	*d*	0.31	*d*	−0.35	*d*	0.39	*d*	0.39	*d*	0.73	*d*	0.56
Al	−0.11	−0.10	−0.42	−0.48	0.71	0.76	−0.61	−0.64	0.32	0.31	0.32	0.31	0.34	0.33	0.55	0.52
Ga	−0.07	−0.07	−0.24	−0.30	0.62	0.67	−0.56	−0.60	0.28	0.26	0.28	0.26	0.35	0.34	0.55	0.51
In	−0.11	−0.14	−0.37	−0.44	0.66	0.72	−0.57	−0.61	0.29	0.29	0.29	0.29	0.31	0.30	0.56	0.53
Tl	−0.06	−0.08	−0.23	−0.30	0.58	0.64	−0.52	−0.57	0.24	0.21	0.24	0.21	0.31	0.30	0.56	0.52
							Complexes [Pd(ECH$_3$)$_4$]									
B	0.06	0.02	0.24	0.20	0.27	0.30	−0.33	−0.35	0.40	0.38	0.40	0.38	0.73	0.73	0.61	0.60
Al	−0.13	−0.10	−0.49	−0.50	0.74	0.77	−0.62	−0.64	0.28	0.26	0.28	0.26	0.35	0.34	0.46	0.44
Ga	−0.10	−0.11	−0.37	−0.40	0.66	0.70	−0.67	−0.60	0.25	0.23	0.25	0.23	0.36	0.35	0.46	0.43
In	−0.14	−0.18	−0.56	−0.59	0.72	0.77	−0.58	−0.62	0.25	0.23	0.25	0.23	0.31	0.30	0.47	0.45
Tl	−0.11	−0.13	−0.43	−0.46	0.64	0.69	−0.53	−0.58	0.19	0.17	0.19	0.17	0.31	0.30	0.45	0.42
							Complexes [Pt(ECH$_3$)$_4$]									
B	0.09	0.05	0.37	0.35	0.23	0.24	−0.32	−0.33	0.43	0.41	0.43	0.41	0.77	0.78	0.69	0.68
Al	−0.17	−0.16	−0.69	−0.69	0.77	0.80	−0.60	−0.63	0.29	0.29	0.29	0.29	0.36	0.36	0.49	0.48
Ga	−0.15	−0.15	−0.58	−0.60	0.69	0.72	−0.54	−0.58	0.26	0.25	0.26	0.25	0.36	0.36	0.49	0.47
In	−0.20	−0.16	−0.78	−0.81	0.75	0.79	−0.56	−0.59	0.26	0.25	0.26	0.25	0.30	0.30	0.49	0.48
Tl	−0.17	−0.13	−0.68	−0.69	0.67	0.71	−0.50	−0.54	0.21	0.20	0.21	0.20	0.30	0.29	0.47	0.46
							Free Ligand ECH$_3$[c]									
B					0.47	0.48	−0.47	−0.48	0.03	0.03	0.03	0.03	0.70	0.71		
Al					0.73	0.74	−0.73	−0.74	0.01	0.01	0.01	0.01	0.37	0.37		
Ga					0.69	0.70	0.69	−0.70	0.01	0.01	0.01	0.01	0.40	0.40		
In					0.69	0.71	−0.69	−0.71	0.01	0.01	0.01	0.01	0.39	0.39		
Tl					0.66	0.68	−0.66	−0.68	0.01	0.00	0.01	0.00	0.40	0.39		

[a] Partial charges q, p-orbital population, Wiberg bond indices P. [b] $p(\pi)$-AO of atom E which is perpendicular to the TM−E−C axis. [c] Calculated using the frozen geometries in the complexes; identical values have been found in the free ligands for all complexes of Ni, Pd, and Pt. [d] No SCF convergence.

sum of the TM−E donor−acceptor interactions leads to a degree of covalent bonding that is less than a single bond. The calculated bond orders for the TM−E bond are always < 0.7 (Table 14). It follows that the high bond dissociation energies are largely caused by charge attraction. The NBO data show that the ligand atoms E always carry a positive partial charge, while the transition metals are negatively charged except in the borylene complexes (Table 14). The positive atomic charges at TM and boron in [TM(BCH$_3$)$_4$] might lead to the wrong conclusion that the charge interactions between TM and boron are repulsive. We want to point out that the charge distribution of the electronic charge around the atoms is highly anisotropic. This may lead to strongly attractive Coulomb interactions even between atoms that carry positive partial charges. For example, the interactions between CO and positively charged transition metals are mainly caused by Coulombic attraction, although the carbon atom of CO carries a positive partial charge.[29]

4. Summary and Conclusion

The results of this study give a comprehensive picture about the bonding situation in transition metal com-

(29) (a) Lupinetti, A. J.; Fau, S.; Frenking, G.; Strauss, S. H. *J. Phys. Chem. A* **1997**, *101*, 9551. (b) Diefenbach, A.; Bickelhaupt, M. F.; Frenking, G. *J. Am. Chem. Soc.*, submitted.

Table 15. NBO and CDA Data of [TM(ECH$_3$)$_4$] at BP86//II and B3LYP/II[a]

	Δq(E)		Δq_π(E)		Δq_σ(E)		Δq (CH$_3$)		d(H$_3$CE→TM)		b(H$_3$CE←TM)	
E	BP86	B3LYP	BP86	B3LYP	BP86	B3LYP	BP86	B3LYP	BP86	B3LYP	BP86	B3LYP
						Complexes [Ni(ECH$_3$)$_4$]						
B	*b*	−0.17	*b*	−0.72	b	+0.55	*b*	+0.13	0.665	0.670	0.505	0.482
Al	−0.02	+0.02	−0.62	−0.60	+0.60	+0.62	+0.12	+0.10	0.554	0.597	0.501	0.461
Ga	−0.07	−0.03	−0.54	−0.50	+0.47	+0.47	+0.13	+0.10	0.586	0.604	0.446	0.410
In	−0.03	+0.01	−0.56	−0.56	+0.59	+0.57	+0.12	+0.10	0.513	0.526	0.418	0.384
Tl	−0.08	−0.04	−0.46	−0.42	+0.54	+0.46	+0.14	+0.10	0.454	0.470	0.404	0.368
						Complexes [Pd(ECH$_3$)$_4$]						
B	−0.20	−0.18	−0.74	−0.70	+0.54	+0.52	+0.14	+0.13	0.675	0.680	0.575	0.551
Al	+0.01	+0.03	−0.54	−0.50	+0.55	+0.53	+0.11	+0.10	0.551	0.563	0.561	0.552
Ga	−0.03	+0.00	−0.48	−0.44	+0.45	+0.44	+0.02	+0.10	0.536	0.541	0.468	0.429
In	+0.03	+0.06	−0.48	−0.44	+0.51	+0.50	+0.11	+0.11	0.425	0.432	0.389	0.364
Tl	−0.02	+0.01	−0.36	−0.34	+0.34	+0.35	+0.13	+0.10	0.413	0.525	0.368	0.329
						Complexes [Pt(ECH$_3$)$_4$]						
B	−0.24	−0.24	−0.80	−0.76	+0.56	+0.52	+0.15	+0.15	0.645	0.650	0.633	0.610
Al	+0.04	+0.06	−0.56	−0.56	+0.60	+0.62	+0.13	+0.11	0.619	0.639	0.553	0.551
Ga	0.00	+0.02	−0.50	−0.48	+0.50	+0.50	+0.15	+0.12	0.571	0.576	0.496	0.494
In	+0.06	+0.08	−0.50	−0.48	+0.56	+0.56	+0.13	+0.09	0.480	0.488	0.401	0.402
Tl	+0.01	+0.03	−0.40	−0.40	+0.41	+0.43	+0.16	+0.14	0.487	0.508	0.365	0.361

[a] Change partial charges q, difference of the π-population and the σ-charges of the atom E between the complexes and the free ligands Δq_π and Δq_σ; positive values indicate that the electronic charge decreases; negative values indicate that the electronic charge increases; charge donation d and back-donation b. [b] No SCF convergence.

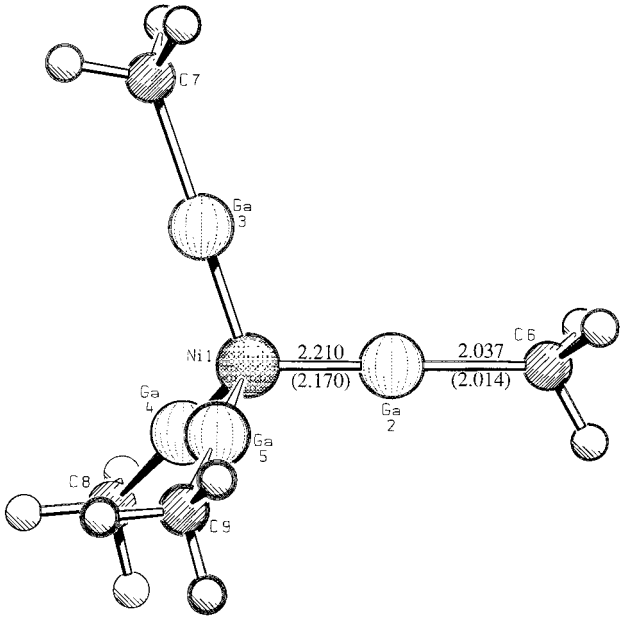

Figure 7. Optimized geometry at BP86/II of [Ni(GaCH$_3$)$_4$]. Bond lengths are given in angstroms. Experimental values are given in parentheses.

plexes with terminal group-13 diyl ligands. The most important conclusions about the TM−ER interactions can be summarized as follows.

(a) The TM−ER bond dissociation energies are very high. Substituents R that are weak π-donors lead to particularly strong TM−ER bonds. The calculated bond energies show the order B > Al > Ga ≈ In > Tl.

(b) The TM−ER bonds are mainly caused by charge attraction between the negatively charged TM atoms and the positively charged group-13 atoms. Covalent contributions to the TM−ER bonds are less important than Coulombic interactions. The TM−ER bond order is in all cases < 1.

(c) The TM←ER σ-donation is clearly larger than the TM→ER π-back-donation when R is a strong π-donor. TM→ER π-back-donation becomes larger and may even become bigger than the TM←ER σ-donation when R is a weak π-donor. The NBO data show that the trend of the TM→ER π-back-donation is in most cases B > Al > Ga > In > Tl, while the TM←ER σ-donation has an irregular sequence. AlR is always the strongest σ-donor and TlR is the weakest σ-donor, while BR, GaR, and InR have similar σ-donor strength.

The results presented here show that a discussion about the question whether the TM−ER bonds should be considered as single bonds or triple bonds is meaningless. The TM←ER π-back-donation may indeed become as important as the TM→ER σ-donation, but the sum of the covalent interactions do not even give a bond order 1. This is different from the bonding situation in TM carbyne complexes, where the bond order for the LnTM−CR bond is between 1.7 and 2.1 for Fischer-type carbyne complexes, and even between 2.3 and 2.5 for Schrock-type carbyne complexes.[9] Thus, [(CO)$_4$FeGaAr*] is not a "ferrogallyne".[5] However, drawing a Lewis structure of the molecule with an Fe−Ga single bond is also not an appropriate representation of the bonding situation.[10] The problem lies in the weakness of the graphical representation of the bond in terms of electron-pair bonding. A triple-bond notation would be appropriate if only the covalent contributions to the Fe−EAr* bond are sketched, which are, however, only a minor part of the iron−gallium bonding interactions.

Acknowledgment. G.F. thanks Professors R. A. Fischer (Bochum) and W. Uhl (Oldenburg, now Marburg) for stimulating discussions and helpful information. This work was supported by the Deutsche Forschungsgemeinschaft and the Fonds der Chemischen Industrie. Excellent service by the Hochschulrechenzentrum of the Philipps-Universität Marburg is gratefully acknowledged. Additional computer time was provided by the HLRZ Stuttgart and the HHLRZ Darmstadt.

OM990936K